Role of Atmospheric Oxygen for the Polymerization of Interleaved Aniline Sulfonic Acid in LDH

El Mostafa Moujahid, Marc Dubois, Jean-Pierre Besse, and Fabrice Leroux*

Laboratoire des Matériaux Inorganiques, CNRS-UMR no. 6002, Université Blaise Pascal, 63177 Aubière Cédex, France

Received January 14, 2002. Revised Manuscript Received May 22, 2002

New polymer/inorganic hybrid materials have been prepared by a two-step soft chemistry route including the intercalation of aniline sulfonic acid between the sheets of a layered double hydroxide (LDH), $Cu_2Cr(OH)_6Cl{\cdot}nH_2O$, and its in situ polymerization at temperatures below 473 K in air atmosphere. A combination of techniques, including X-ray diffraction, X-ray absorption spectroscopy at Cu, Cr, and S K-edge, electron spin resonance, and infrared spectroscopies, was used for their characterization. For the first time, a pure nanocomposite was successfully obtained. The interleaved polymer is found to be present under its emeraldine salt form. In situ ESR measurements enable determination of the thermal condition for the polymerization, showing the kinetic factor of the process. Like other lamellar nanocomposites, the atmospheric oxygen plays a major role for the polymerization process, although, here it is crucial, since no redox chemistry or external oxidizing agents are employed. The monomer confinement and its matching with the layer charge density of the host framework are found to be of great importance.

1. Introduction

A great interest is devoted to nanocomposites prepared from the assembly of an organic polymer and an inorganic lamellar structure.[1] The present paper deals with the inorganic/organic nanocomposite materials and more specifically on those containing conjugated polymer as the organic moiety. It may be of interest for potential application in electrocatalysis.[2] From the point of view of the inorganic structure, the polymer provides the conductive properties, enhancing the diffusion of species. Alternatively, the inorganic framework supplies a confinement and a mechanical strength for the whole.

Layered double hydroxide (LDH) material is taken as the 2D-host framework. LDH materials provide some potential applications as a clay-modified electrode after the encapsulation of electroactive molecules.[3] Large anions such as polyoxometalate,[4] DNA molecule,[5] and organic[1d,6] or inorganic polymers,[7] have been intercalated between the LDH sheets. Hydrotalcite-like LDH materials are described according to the ideal formula $[M^{II}_{1-x}M_x^{III}(OH)_2]^{x+}_{intra}[A^{m-}_{x/m}{\cdot}nH_2O]_{inter}$, where M^{II} and M^{III} are metal cations, A the anions, and "intra" and "inter" denote the intralayer and interlayer domain, respectively. The structure consists of brucite-like layers constituted of edge-sharing octahedra.[8] The presence of trivalent cations induces a positive charge in the layers, which is balanced by interlamellar anions.

Polyaniline (PANI) was chosen as the organic moiety. This polymer has been successfully intercalated in several host materials, such as V_2O_5 xerogel,[9] MoO_3 bronze,[10] graphitic oxide,[11] and α-$RuCl_3$,[12] and in three-dimensional matrixes, such as zeolites.[13] PANI/LDH nanocomposite was first reported by Challier and Slade.[14] Prior to the incorporation, the LDH host structure was exchanged with terephthalate or hexacyanoferrate anions in order to expand the basal spacing. The preswollen LDH materials were then refluxed under pure aniline. Although, it gives rise to ill-defined samples. More recently, it was shown that the polymerization reaction may occur in the gallery of the $LiAl_2(OH)_6Cl{\cdot}H_2O$ hydrotalcite-type compound using mild conditions.[15] A thermal treatment at 263 K for 10 days was performed on the LDH matrix after the incorporation of aniline carboxylic acid. However, the material was not pure, since the diffraction peaks of the pristine material remain present.[15]

* Corresponding author. E-mail: fleroux@chimtp-univ.bpclermont.fr.

(1) (a) Komarni, S. *J. Mater. Chem.* **1992**, *2*, 1219. Ruiz-Hitzky, E. *Adv. Mater.* **1993**, *5*, 334 (b) Giannelis, E. *Adv. Mater.* **1996**, *8*, 29. Novak, B. M. *Adv. Mater.* **1993**, *5*, 422 (c) Ishida H.; Campbell, S.; Blackwell, J. *Chem. Mater.* **2000**, *12*, 1260 (d) Leroux, F.; Besse, J.-P. *Chem. Mater.* **2001**, *13*, 3507.

(2) Shaw, B. R.; Creasy, K. E. *J. Electroanal. Chem.* **1988**, *243*, 209.

(3) Itaya, K.; Chang, H.-C.; Uchida, I. *Inorg. Chem.* **1987**, *26*, 624.

(4) Dimotakis, E. D.; Pinnavaia, T. J. *Inorg. Chem.* **1990**, *13*, 2393.

(5) Choy, J.-H.; Kwak, S.-Y.; Park, J.-S.; Jeong, Y.-J.; Portier, J. *J. Am. Chem. Soc.* **1999**, *121*, 1399.

(6) Oriakhi, C. O.; Farr, I. V.; Lerner, M. M. *J. Mater. Chem.* **1996**, *6*, 103.

(7) Yun, S. K.; Constantino, V. R. L.; Pinnavaia, T. J. *Clays and Clay Miner.* **1995**, *43*, 503. Depège, C.; El Metoui, F.-Z.; Forano, C.; de Roy, A.; Dupuis, J.; Besse, J.-P. *Chem. Mater.* **1996**, *8*, 952.

(8) De Roy, A.; Forano, C.; El Malki, K.; Besse, J.-P. *Synthesis of Microporous Materials*; Occelli, L., Robson, H., Eds.; Van Nostrand, Reinhold **1992**, *2*, 108.

(9) Kanatzidis, M. G.; Wu, C. -G.; Marcy, H. O.; DeGroot, D. C.; Kannewurf, C. R. *Chem. Mater.* **1990**, *2*, 222.

(10) Kerr, T. A.; Wu, H.; Nazar, L. F. *Chem. Mater.* **1996**, *8*, 2005.

(11) Liu, P.; Gong, K. *Carbon* **1999**, *37*, 701.

(12) Wang, L.; Brazis, P.; Rocci, M.; Kannewurf, C. R.; Kanatzidis, M. G. *Chem. Mater.* **1998**, *10*, 3298.

(13) (a) Enzel, P.; Bein, T. J. *J. Phys. Chem.* **1989**, *93*, 6270, (b) Frisch, H. L.; Song, H.; Ma, J.; Rafailovich, M.; Zhu, S.; Yang, N.-L.; Yan, X. *J. Phys. Chem. B* **2001**, *105*, 11901.

(14) Challier, T.; Slade, R. C. T. *J. Mater. Chem.* **1994**, *4*, 367.

(15) Isupov, V. P.; Chupakhina, L. E.; Ozerova, M. A.; Kostrovsky, V. G.; Poluboyarov, V. A. *Solid State Ionics* **2001**, *141−142*, 231.

10.1021/cm0211094 CCC: $22.00
Published on Web 08/09/2002

Table 1. Chemical Compositions of LDH Materials

sample	formulas
$Cu_2Cr(OH)_6/Cl$	$Cu_{0.68}Cr_{0.32}(OH)_2\ Cl_{0.33}\cdot 0.75H_2O$[a]
$Cu_2Cr(OH)_6/ANIS$	$Cu_{0.67}Cr_{0.33}(OH)_2(C_6H_4NH_2SO_3)_{0.32}Cl_{0.003}\cdot 0.68H_2O$
$Cu_2Cr(OH)_6/ANIS$ (473 K)	$Cu_{0.67}Cr_{0.33}(OH)_2(C_6H_4NH_2SO_3)_{0.32}Cl_{0.003}\cdot 0.33H_2O$

[a] Associated with an anionic exchange capacity of 286 mequiv/100 g.

In the present study, the incorporation and the polymerization of aniline sulfonic acid (ANIS) between the sheets of the $Cu_2Cr(OH)_6Cl\cdot H_2O$ hydrotalcite-type material are reported. The presence of Cu^{2+} cations added to the layers corrugation make $Cu_2Cr(OH)_6Cl\cdot H_2O$ material an attractive host structure.[16] For the monomer, the electrophilic function decreases the potential of polymerization,[17] and the sulfonic acid ring-substituted polyaniline (PANIS) is capable of self-doping.[18] This is suitable, since any doping using an external oxidizing agent induces preferentially an exchange with the counteranions.[19] It explains the choice of a thermal treatment. The conductivity of PANIS is independent of the external protonation over a broad pH range, although the presence of the sulfonate groups decreases the conductivity of the polymer in its conductive state.[20]

The nanocomposite is characterized by a combination of techniques. The information relative to the long-range order is provided by XRD and the local environment surrounding both transition metals (Cu and Cr cations) by EXAFS study. XANES at the sulfur K-edge was employed to characterize the sulfonate function. The oxidation state of the polymer was estimated by FTIR, and the temperature of the heat treatment was optimized by ESR spectroscopy.

Isupov et al. surmise that the air atmosphere may be of importance to trigger the polymerization process and pointed out an eventual role of humidity.[15] To elucidate these questions, in situ ESR measurements were performed under different conditions (air, vacuum). In addition, the kinetics of the reaction was addressed.

2. Experimental Section

2.1. Syntheses. The [Cu_2Cr-Cl] hydrotalcite-like material was prepared by the addition of $CrCl_3$ solution on CuO as described by De Roy et al.[8] Experimentally, 250 mL of $CrCl_3$ (10^{-2} M, hexahydrate form from Aldrich) was added dropwise to a suspension of copper oxide (CuO) (20 mmol, grain size ≈ 5 mm, 99.99%, Aldrich). The slurry is aged overnight, centrifuged, then washed several times with decarbonated water, and finally dried at room temperature.

2.2. Exchange and Polymerization. Exchange with aniline sulfonic acid (*o*-aminobenzenesulfonic acid, 97%, Aldrich) solution was carried out using twice the amount corresponding to the LDH exchange capacity. The exchange reaction time was of 24 h. The resulting powder was washed several times with decarbonated water and then dried at room temperature. For the polymerization reaction, the hybrid phase was placed in an open alumina crucible at 473 K for 4 h under an air atmosphere.

Elemental analysis was performed at the Vernaison Analysis Center of CNRS using inductive conduction plasma coupled to atomic emission spectroscopy (ICP/AES). The chemical compositions are reported in Table 1.

2.3. Instrumentation. Powder X-ray diffraction profiles (PXRD) were obtained with a Siemens D500 X-ray diffractometer with a diffracted beam monochromator Cu Kα source. Steps of 0.04° with a counting time of 4 s were used. X'Pert Pro Philips equipped with a HTK16 Anton Paar chamber and a PSD-50m Braun detector was used to record XRD diagrams at various temperatures. The conditions were as follows: step width of 0.0387°, time per step of 60 s, an aperture on 2° (155 channels).

2.4. Electron Spin Resonance. ESR spectra were recorded using a X Band Bruker EMX spectrometer equipped with a standard variable-temperature accessory and operating at 9.653 GHz at room temperature and at 9.411 GHz when the temperature accessory was set up. Diphenylpicrylhydrazyl (DPPH) was used to determine the resonance frequency ($g = 2.0036 \pm 0.0002$).

2.5. X-ray Absorption Spectroscopy. *2.5.1. Cu and Cr K-Edge.* An EXAFS (extended X-ray absorption fine structure) study was performed at LURE (Orsay, France) using X-ray synchrotron radiation emitted by the DCI storage ring (1.85 GeV positrons, average intensity of 250 mA) at the D44 beam line. Data were collected at 10 K in transmission mode at both Cr and Cu K-edge (5989.2 and 8978.9 eV, respectively). A double-crystal Si(111) monochromator was used for energy selection with a two-mirror device for harmonic rejection for the spectra at the Cr K-edge. The absorption is detected using He/Ne/air-filled ion chambers. The energy is scanned using steps of 2 eV from 100 eV below to 900 eV above both K-edges with an accumulation time of 2 s per point. Three spectra were recorded for each sample.

2.5.2. S K-Edge. XANES (X-ray absorption near edge structure) spectra were recorded at the SA32 beamline at LURE, using the SuperAco positron storage ring (800 MeV, ≈173 mA). The beamline was equipped with a Ge(III) double crystal monochromator. The experiments were performed at room temperature in total yield electron mode. The energy was calibrated against the edge threshold position for ZnS (first intense peak on the first derivative dAbs vs dE curve calibrated at 2473.0 eV). Two spectra were recorded from 2460 to 2560 eV with a step of 0.2 eV and 1 s of accumulation per point.

2.6. EXAFS Analysis. Standard procedures for the extraction and the normalization of the signal are presented elsewhere.[21] EXAFS spectra are treated according to the classical plane-wave single scattering approximation. The Fourier transforms of EXAFS spectra were obtained after multiplication of the signal by a k^3 factor over a 2.8−12.5 Å^{-1} Kaiser apodization window with $t = 2.5$. The $\chi(k)$ signal was fitted using the formula $\chi(k) = S_0^2\sum A_i(k)\ \sin[2kr_i + \phi_i(k)]$, with the amplitude $A_i(k) = (N_i/kr_i^2)F(k)\ \exp(-2k^2\sigma_i^2)$, where r_i is the interatomic distance, ϕ_i the total phase shift of the ith shell, N_i the effective coordination number, σ_i the Debye−Waller factor, and $F_i(k)$ the backscattering amplitude. EXAFS signal treatments and refinements were performed using an available program package.[22] The residual ρ factor is defined as $\rho =$

(16) Roussel, H.; Briois, V.; Elkaim, E.; de Roy, A.; Besse, J.-P. *J. Phys. Chem. B* **2000**, *104*, 5915.
(17) Wei, X.; Epstein, A. J. *Synth. Met.* **1995**, *74*, 123. Kuramoto, N.; Geniès, E. M. *Synth. Met.* **1995**, *68*, 191.
(18) Chen, S.-A.; Hwang, G.-W. *Polymer* **1997**, *38*, 3333; Tang, H.; Kitani, A.; Yamashita, T.; Ito, S. *Synth. Met.* **1998**, *96*, 43; Wei, X.; Epstein, A. J. *Synth. Met.* **1995**, *74*, 123.
(19) Rey, S.; Mérida-Robles, J.; Han, K. −S.; Guerlou-Demourgues, L.; Delmas, C.; Duguet, E. *Polym. Int.* **1999**, *48*, 277.
(20) Yue, J.; Wang, Z. H.; Cromack, K. R.; Epstein, A. J.; MacDiarmid, A. G. *J. Am. Chem. Soc.* **1991**, *113*, 2665.
(21) Leroux, F.; Piffard, Y.; Ouvrard, G.; Mansot, J. -L.; Guyomard, D. *Chem. Mater.* **1999**, *11*, 2948.
(22) Michalowicz, A. *Round Midnight, EXAFS Signal Treatment and Refinement Programs*, LURE, Orsay, France. Programs available on LURE Web site; http://www.LURE.fr.

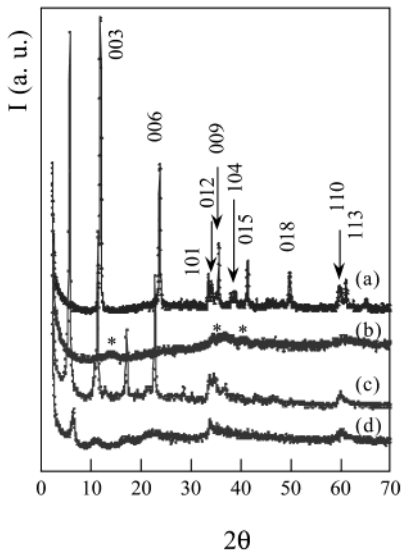

Figure 1. XRD patterns of LDH materials and derivatives: $Cu_2Cr(OH)_6/Cl$ at (a) room temperature and (b) after a treatment at 200 °C, $Cu_2Cr(OH)_6$/ANIS at (c) room temperature and (d) after a treatment at 200 °C. Cu_2OCl_2 is designed as *. Patterns are offset for clarity.

$[\Sigma(k^3\chi_{exp}(k) - k^3\chi_{theo}(k))^2/\Sigma(k^3\chi_{exp}(k))^2]^{1/2}$. The commonly accepted fitting accuracy is about 0.02 Å for the distance and 15−20% for the number of neighboring atoms.

3. Results and Discussion

3.1. Characterization of the Nanocomposite. *3.1.1. Exchange Reaction.* The powder X-ray diffraction pattern of $Cu_2Cr(OH)_6Cl{\cdot}2.25H_2O$ (=$Cu_{0.66}Cr_{0.33}(OH)_2Cl_{0.33}{\cdot}0.75H_2O$) is characteristic of the layered double hydroxide structure; Miller indexing is given in Figure 1. The pattern was refined using $R\bar{3}m$ space group in rhombohedral symmetry (eight distinct d_{hkl} distances were indexed). The cell parameters a and c (equal to 3 times the interlamellar distance) are equal to 0.311 and 2.315 nm, respectively. Since (101) and (102) contributions are relatively strong, the pristine phase may present a mixture of polytypes.[23] An additional diffraction peak at $2\theta = 36°$ may be due to a change to a lower symmetry ($P3_1$), although the small intensity makes difficult any refinement.

The exchange by the monomer increases the d spacing from 0.772 to 1.560 nm. It is consistent for the presence of two monomer layers in the interlamellar domain. No diffraction peak of the pristine material is observed. In comparison, the incorporation of the monomer (ANIC) between the layers of $LiAl_2(OH)_6Cl{\cdot}H_2O$ is not complete, leaving a large portion of the pristine material intact.[15] The coherence length along the stacking direction was estimated using the Scherrer formula: $D_{hkl} = 0.9\lambda/\beta_{1/2}\cos\theta$, in which λ is the X-ray wavelength, θ the diffraction angle, and $\beta_{1/2}$ the width at half-maximum intensity. A domain of 1080 Å was found for the pristine material, it corresponds to ≈140 stacked layers, close to what is observed for other well-crystallized LDH materials.[8] This is slightly greater than that of the hybrid phase, 920 Å (corresponding to ≈60 stacked layers).

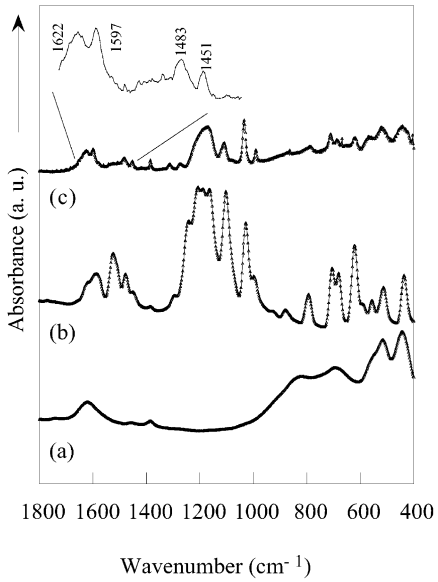

Figure 2. IR spectra of (a) $Cu_2Cr(OH)_6/Cl$, (b) ANIS monomer, and (c) $Cu_2Cr(OH)_6$/PANIS nanocomposite. A selective region is displayed in inset (see the text).

3.1.2. Polymerization. Previous work on the PANI/MoO_3 system has shown that the in situ polymerization is possible when utilizing an external oxidizing agent.[10] The reaction time is of importance, since the most highly crystalline phase was obtained after only 0.5 h; longer time gives rise to an oxidation of the framework and to the formation of byproducts. In our case and like other authors' observation,[19] any attempt to polymerize chemically the interleaved monomer was unsuccessful, leading to a partial exchange with the agent counteranions. Taking advantage of the ring-substituted aniline being easier to polymerize electrochemically than the pure aniline and in order to leave the 2D character intact, a soft thermal treatment is utilized.

In situ polymerization was reached after a thermal treatment at 473 K for 4−8 h. From pale green, the nanocomposite color turns to dark brown. The diffraction peaks of the nanocomposite become broader, whereas the pristine material transforms into the copper oxichloride Cu_2OCl_2 (Figure 1). The interlayer distance decreases slightly to 1.402 from 1.560 nm, showing that a reorientation of the interlamellar species occurs. This phenomenon is usually observed in the case of an in situ polymerization, as illustrated by the polymerization of ϵ-aminocaproic acid to nylon into α-ZrP,[24] and acrylate[19,25] or α,β aspartate[26] into hydrotalcite type compounds. The coherence length along the stacking direction (vide supra) is greatly diminished, reaching the limit of validity for the Scherrer relation.

3.1.3. Oxidation State of the Polymer. To know if the mild heat treatment induces the polymerization, a combination of techniques was used to address the issue. FTIR is utilized because it may estimate the intrinsic oxidation state of PANI and address the interaction between the polymer and the LDH host framework. It

(23) Newman, S. P.; Jones, W.; O'Connor, P.; Stamines, N. *J. Mater. Chem.* **2002**, *12*, 153.

(24) Ding Y.; Jones, D. J.; Maireless-Torres, P.; Rozière, J. *Chem. Mater.* **1995**, *7*, 562.

(25) Tanaka, M.; Park, I. Y.; Kuroda, K.; Kato, C. *Bull. Chem. Soc. Jpn.* **1989**, *62*, 3442.

(26) Whilton, N.T; Vickers, P. J.; Mann, S. *J. Mater. Chem.* **1997**, *7*, 1623.

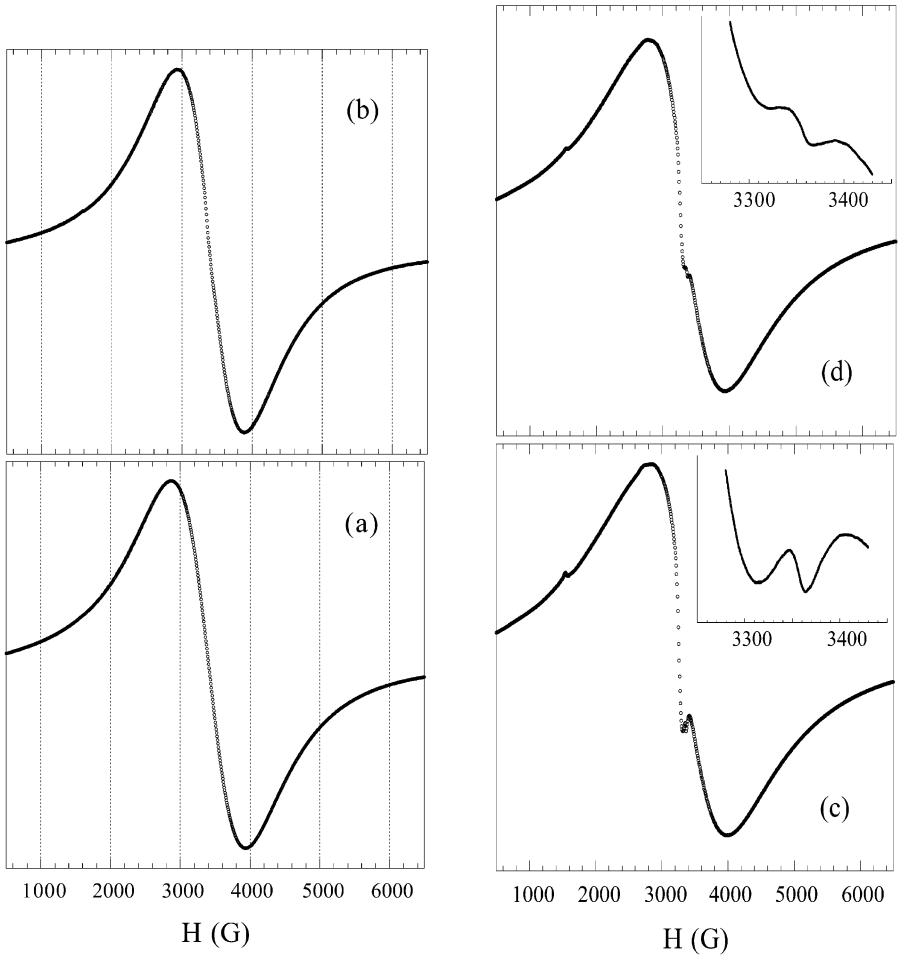

Figure 3. Derivative of the ESR signal for (a) $Cu_2Cr(OH)_6/Cl$, (b) $Cu_2Cr(OH)_6$/ANIS, and $Cu_2Cr(OH)_6$/PANIS at (c) 130 K and (d) 300 K. Inset: the $Cu_2Cr(OH)_6$/PANIS spectra was recorded with a sweep width of 150 G to magnify the narrow signal (receiver gain, 5000).

has been employed for many nanocomposite systems.[6,9,10,13,15] In our case, the presence of PANIS is supported by the vibration bands at 1597 and 1483 cm^{-1} (Figure 2), which are characteristic of the ring mode of quinoid and phenyl-nitrogen, respectively. It shows that PANIS is present under its emeraldine salt or base form.[27] However, the vibration of the $\nu_2(H_2O)$ band at 1620 cm^{-1} makes difficult a quantitative estimation of the oxidation state of the polymer. Comparatively, it is higher than that of other relative hybrid phases,[14] being between values reported for PANI/MoO_3[10] and PANI/$RuCl_3$[12] nanocomposites. The broad vibration band localized at 1170 cm^{-1} is ascribed to the presence of para-substituted aromatic C−H (δ in plane) and to the aromatic C−N (υ). They are localized at 1150 and 1265 cm^{-1} for PANI, respectively. For δ_{C-H}, the shift for PANIS provides a measure of the extent of the electron delocalization.[28] The vibration bands at 1108 and 1034 cm^{-1} are characteristic of the vibrations of the sulfur atoms linked to the aromatic cycle and of S═O symmetric, respectively.[29] The $S{=}O_{asym}$ vibration is observed at 1179 cm^{-1}. A shift of 8 cm^{-1} to higher frequency is observed for the S═O vibration band after the polymerization; it is transmitted also to the C−S band. The inorganic lattice vibrations appear in the 400−650 cm^{-1} wavenumber range.

Electron spin resonance (ESR) spectroscopy is known to be a powerful tool to characterize the spin carriers in doped and undoped conducting polymers.[30] The ESR spectra of the pristine and monomer-exchanged material (Figure 3a,b) exhibit a single Gaussian line with a peak-to-peak line width, noted as ΔH_{pp}, close to 1100 ± 20 G (g = 2.0621± 0.0005). The line shape is attributed to the combination of paramagnetic ions $Cu^{2+}(3d^9)$ and $Cr^{3+}(3d^3)$ in the material. An additional narrow signal is observed for the nanocomposite with the following characteristics: ΔH_{pp} = 17 ± 2 G at 130 K and ΔH_{pp} = 30 ± 4 G at 300 K. Since some uncertainties may arise from the estimation of the line width and of the associated g value, the experiments are reproduced using a smaller field range (see the inset of Figure 3c,d). The g value of the narrow signal (g = 2.0034 ± 0.0004)

(27) Shacklette, L. W.; Wolf, J. F.; Gould, S.; Baughman, R. H. *J. Chem. Phys.* **1988**, *88*, 3955.
(28) Chiang, J. C.; MacDiarmid, A. G. *Synth. Met.* **1986**, *13*, 193.
(29) Leroux, F.; Adachi-Pagano, M.; Intissar, M.; Chauvière, S.; Forano C.; Besse, J.-P. *J. Mater. Chem.* **2001**, *11*, 105.

(30) (a) Houzé, E.; Nechtschein, M.; Travers, J. P. *Phys. Rev. B* **1996**, *53*, 14309. (b) Kispert, L. D.; Joseph, J.; Miller, G. G.; Baughman, R. H. *J. Chem. Phys.***1984**, *81*, 4. (c) Zhuang, L.; Zhou, Q.; Lu, J. *J. Electranal. Chem.* **2000**, *493*, 135. (d) Dubois, M.; Merlin, A.; Billaud, D. *Solid State Com*, **1999**, *11*, 571. (e) Billaud, D.; Ghanbaja, J.; Marêché, J. F.; Mc Rae, E.; Goulon, C. *Synth. Met.* **1989**, *28*, 147. (f) Rachdi, F.; Bernier, P. *Phys. Rev. B* **1986**, *33*, 11. (g) Mizoguchi, K.; Honda, Kachi, N.; Shimizu, F.; Sakamoto, H.; Kume, K. *Solid State Commun.* **1995**, *96*, 333. (h) Feher, G.; Kip, A. F. *Phys. Rev. B* **1955**, *98*, 337.

Table 2. Characteristics of ESR Signals at 293 K

sample	ΔH_{pp} (G)[a]	g value (±0.0005)
$Cu_2Cr(OH)_6/Cl$	1100 ± 20	2.0621
ANIS	undetectable	
$Cu_2Cr(OH)_6$/ANIS	1100 ± 20	2.0621
$Cu_2Cr(OH)_6$/PANIS	1100 ± 20	2.0621
	30 ± 2	2.0034

[a] Peak-to-peak line width.

is typical of organic radicals and/or conduction electrons. Absent in the pristine and in the monomer-exchanged materials, the additional narrow line is then attributed to the spin carriers localized along the polymer chains. PANI intercalated in layered perovskite shows an ESR signal at $g = 2.004$[31] similar to that of bulk polyaniline ($g = 2.0034$).[13] ESR data are displayed in Table 2. It is interesting to note that the monomer ANIS gives no detectable signal, even after a heat treatment at 473 K. The polymerization occurs only using an oxidizing agent under high-pressure condition (7 kbar).[32] It underlines the importance of the confinement provided by the LDH framework for the polymerization reaction.

The broadening of the large signal is due to different types of interactions (dipolar, exchange, etc.) between the paramagnetic ions present in high concentration. The isotropic signal is insensitive to the temperature in the range 130−300 K (Figure 4), whereas the narrow line presents a linear dependence on the temperature. The evolution of the line width is displayed in Figure 4. This behavior is reported for other doped conducting polymers such as polyparaphenylene,[30d] polyacetylene,[30e,f] polypyrole, and polythiophene.[30g] The positive temperature dependence of the ESR line width is typical of conduction electrons in metals.[30h] It has been related to a relaxation mechanism via spin−orbit interactions of bands, known as the theory of Elliott.[33] To summarize, ΔH_{pp} is proportional to $(\Delta g)^2 T$, where Δg is the deviation between the experimental g factor and the one corresponding to free electron ($g = 2.0023$). Our results suggest that a large portion of the polymer exhibits a metallic character and the spin carriers are the conduction electron. In comparison, ΔH_{pp} does not present a linear temperature dependence for the ANIC/Li_2Al LDH system.[15]

3.1.4. EXAFS Study. Since the thermal treatment gives rise to weak nonbasal reflections, no information relative to the intralamellar arrangement is provided. To shed some light, XAS experiments were performed. The local environment around Cr and Cu cations are examined and the interactions between the organic moiety and the inorganic sheets are addressed. The sulfur K-edge XANES curves are displayed in Figure 5. The spectra are dominated by a single white-line feature reflecting the transitions from 1s to *n*p and corresponding to localized, unfilled atomic or molecular states. The white line is slightly shifted after the intercalation of the monomer. It is explained by the interaction of the sulfonate groups with the inorganic host structure. After the treatment at 473 K, the shift is much larger (≈2 eV). The energy is then close to the one observed for sodium dodecyl sulfate surfactant

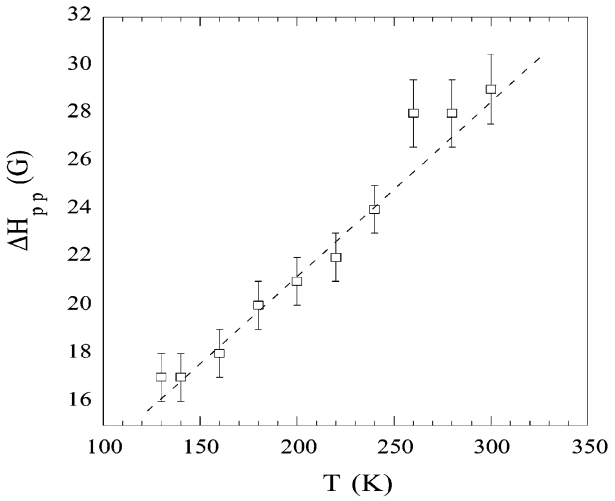

Figure 4. Variation of the peak-to-peak ESR line width ΔH_{pp} vs T for $Cu_2Cr(OH)_6$/PANIS nanocomposite.

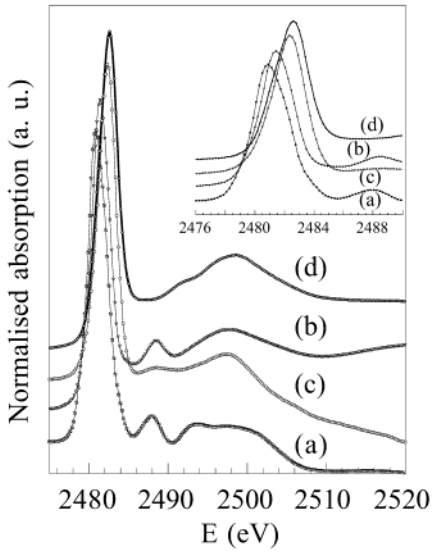

Figure 5. Sulfur XANES K-edge spectra for (a) ANIS monomer, (b) $Cu_2Cr(OH)_6$/ANIS, (c) $Cu_2Cr(OH)_6$/PANIS, and (d) Na-DS. The white-line region is enlarged in the inset.

molecule, in which the sulfur atoms are located in a C_{3v} oxygen environment. It means that the sulfur atoms are present under a more oxidized state after the thermal treatment. It may be explained by a grafting process, further supported by the shift of the S═O vibration band observed in the FTIR spectra (Figure 2).

For both cations' K-edge, the moduli of the Fourier transforms are displayed in Figure 6. The first peak is assigned to the first oxygen atom cage and the second to the metals neighboring the central atom. Since the curves are superimposable, the close environment surrounding the two cations is not modified by the reaction of polymerization. The refinements are in agreement with what was previously observed by other authors (Table 3)[16] and consistent for local order.[34] The multiple scattering amplified in the case of three atoms lining up [35] and usually observed for LDH materials [36] is absent for the pristine and the organic derivative

(31) Uma, S.; Gopalakrishnan, J. *Mat. Sci. Eng. B* **1995**, *34*, 175.
(32) Chan, H. S. O.; Neuendorf, A. J.; Ng, S.-C.; Wong, P. M. L.; Young, D. J. *Chem. Com.* **1998**, 1327.
(33) Elliot, R. J. *Phys. Rev. B* **1954**, *96*, 266.
(34) Hofmeister, W.; Platen, H. V. *Crystallogr. Rev.* **1992**, *3*, 3.
(35) Alberding, N.; Crozier, E. D. *Phys. Rev. B* **1983**, *27*, 3374.
(36) Leroux, F.; Moujahid, El M.; Taviot-Guého, C.; Besse, J.-P. *Solid State Sci.* **2001**, *3*, 81.

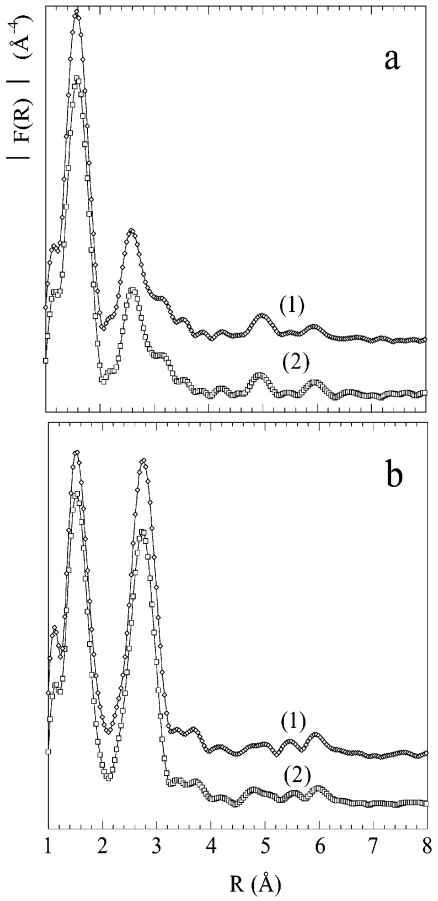

Figure 6. Moduli of the Fourier transform at (a) Cr K-edge for (1) $Cu_2Cr(OH)_6$/Cl LDH phase and (2) $Cu_2Cr(OH)_6$/PANIS, and (b) Cu K-edge for (1) $Cu_2Cr(OH)_6$/Cl LDH phase and (2) $Cu_2Cr(OH)_6$/PANIS. Distances are not corrected from the atomic potential phase shifts.

Table 3. EXAFS Fit Results for $Cu_2Cr(OH)_6$/PANIS

edge	*N* (atom)	*R* (Å)	$\sigma^2 \times 10^{-3}$ (Å^2)	ρ (%)
Cr	6 (O)	1.98	3.2	
	6 (Me)[a]	3.12	8.5	5
Cu	4 (O)	1.98	3.8	
	2 (O)	2.30	6.9	
	6 (Me)[a]	3.12	9.2	3

[a] The two cations (Cu^{2+} and Cr^{3+}) are undistinguishable, as backscatters.

sample. An angular deviation of 10° from the collinear octahedra organization is although enough to attenuate completely the focusing effect.[37] Therefore, the absence of a peak at longer distance is explained by the corrugation of the sheets.

3.1.5. Understanding of the Polymerization Reaction. The polymerization of the ring-substituted PANI and the presence of the quinoid band associated with a conductive state of the polymer in the LDH structure remain difficult to address. In some cases, positive charges localized along the chain of the polymer may correspond to the quinone diimine radical cations or to the polarons obtained by p-doping. For instance, transition metal cations such as Fe^{3+} may interact with the π electrons of the aromatic ring to give rise to the radical cations.[38] This was also speculated for PANI/Cu_2Cr

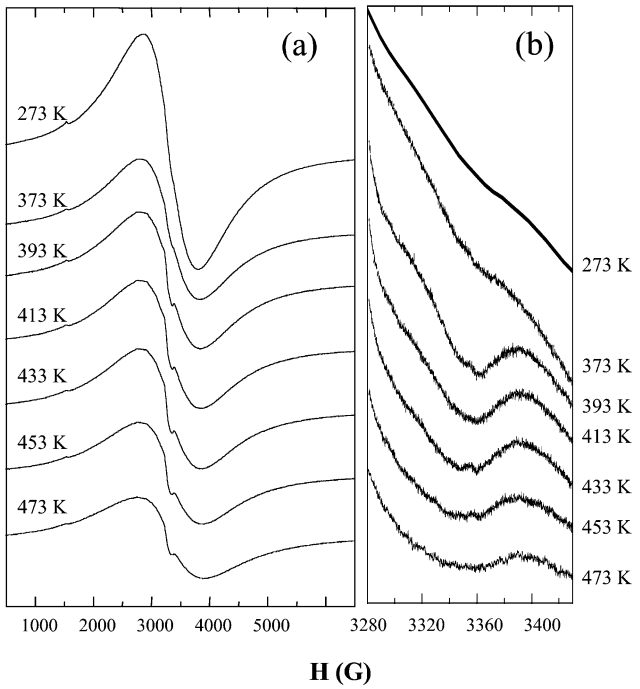

Figure 7. In situ ESR spectra of $Cu_2Cr(OH)_6$/ANIS in the temperature range 273−473 K recorded with a sweep width of (a) 6500 G and (b) 150 G. Receiver gain, 5000.

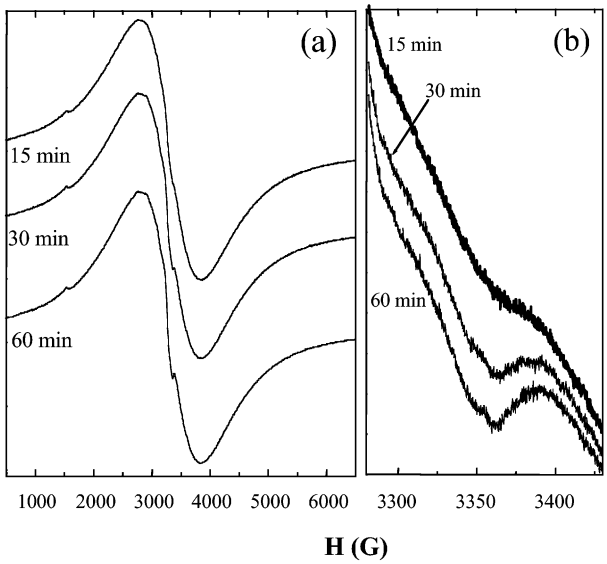

Figure 8. Evolution with time of the ESR lines of $Cu_2Cr(OH)_6$/ANIS LDH hybrid heated at 393 K in air (sweep width, 6500 G (a) and 150 G (b); receiver gain, 10000)).

nanocomposite.[14] The eventual participation of the Cu or Cr cation is discarded, since the shape of the broad signal remains intact. The Cu cations present in the LDH phase as an isolated species or cluster should exhibit a well-resolved hyperfine structure on the ESR signals.[39] We exclude then the possibility of Cu cation migration during the thermal treatment. The recent work of Isupov et al. supports our finding, since they found that the polymerization reaction may occur for the electronic insulator hydrotalcite.[15] The participation

(37) Ressler, T.; Brock, S. L.; Wong, J.; Suib, S. L. *J. Phys. Chem. B* **1999**, *103*, 6407.
(38) Moreale, A.; Closs, P.; Badot, C. *Clay Miner.* **1985**, *20*, 29.
(39) Bahranowski, K.; Dula, R.; Gasior, M.; Labanowska, M.; Michalik, A.; Vartikian, L. A.; Serwicka, E. M. *Appl. Clay Sci.* **2001**, *18*, 93.

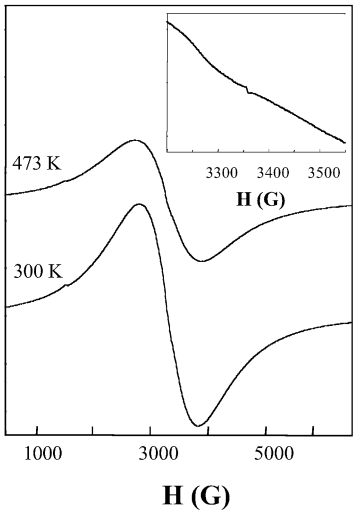

Figure 9. ESR signal of $Cu_2Cr(OH)_6$/ANIS hybrid material at 300 and 473 K under static vacuum condition recorded with a sweep width of 6500 G (250 G in the inset) (receiver gain, 500 000).

of atmospheric oxygen was also hypothesized.[15] To explain the presence of conjugated PANIS units, the reaction was studied by in situ ESR experiments.

ESR spectra using broad (6500 G) and small (150 G) field range were recorded in air atmosphere after 0.5 h at various temperatures ranging from 279 to 473 K (Figure 7). The signal of the polymer is depicted by a fine line at 393 K. A shoulder is also visible at 373 K, indicating an ignition of the polymerization process at lower temperature. As mentioned before, the whole signal is composed of a broad signal associated with the LDH framework and a narrow line relevant to the polymeric portion. The line width (ΔH_{pp}) of the broad signal is independent of the heating process, whereas it increases in temperature for the other signal. The positive dependence of ΔH_{pp} observed in the temperature range 130−300 K is also extended at higher temperature. It confirms the metallic behavior of at least a part of the nanocomposite.

To know if the reaction is kinetically limited, the temperature was set at 393 K for 1 h. Figure 8 displays the evolution of the ESR lines. The fine line due to the polymer increases continuously in intensity without broadening; the associated line width is 40 ± 10 G with $g = 2.0034$. The polymerization reaction is then proved to be kinetically impeded. Lower temperature of treatment is associated with longer time, 373 K for 4 h, giving rise to a similar effect.

ESR experiments were performed under static vacuum (10^{-2} atm). The spectra recorded at 300 and 473 K are identical (Figure 9), except for the decrease in intensity of the broad line. An extremely weak line is observed at 473 K ($\Delta H_{pp} = 6 \pm 1$ G), more than 500 times less intense than the signal obtained in air. Thus, it ascertains the role of the atmospheric oxygen necessary for the polymerization. The participation of the oxygen molecule in the polymerization of PANI was reported for other 2D inorganic systems, although with the use of much longer time. For instance, up to 10 days at 403 K were necessary for layered Brönsted acids of composition $HMMoO_6 \cdot H_2O$ (M = Nb, Ta).[40] First identified by Kanatzidis group,[41] the role of oxygen occurs also in the postintercalative polymerization. Initially induced by an oxidizing agent, the intralamellar polymer growth is facilitated by the molecular oxygen. A postpolymerization reaction is observed in our samples (vide infra).

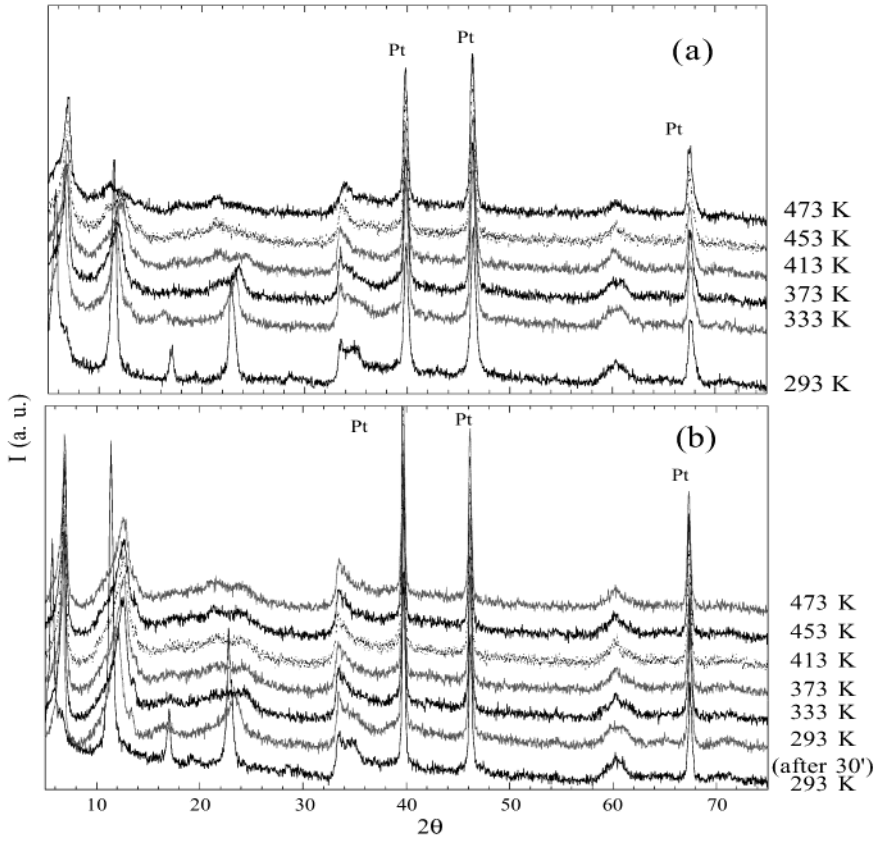

Figure 10. XRD patterns of $Cu_2Cr(OH)_6$/ANIS hybrid material treated in situ under (a) air or (b) vacuum.

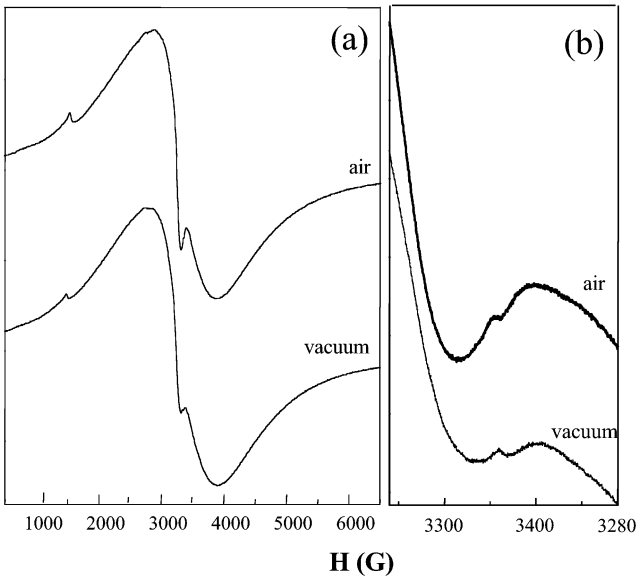

Figure 11. ESR signals of $Cu_2Cr(OH)_6$/PANIS nanocomposite exposed to air for 30 days (noted air) and of the same sample outgassed under dynamic vacuum (noted vacuum) (sweep width, 6500 G (a) and 250 G (b); receiver gain, 10 000).

In situ XRD patterns of ANIS/Cu_2Cr hybrid material are recorded in air or under vacuum (Figure 10). Under vacuum, the basal spacing decreases from 1.560 to 1.435 nm. The contraction of the 2D structure corresponds to a thermal treatment in air at 333 K and is explained by the removal of water molecules from the LDH structure. By comparison with ESR data, we infer that the presence of physisorbed water molecules is not responsible for the polymerization reaction. There are no striking differences between XRD diagrams recorded either in air or under vacuum at higher temperature ($T \leq 473$ K). Under vacuum at 473 K, the basal spacing decreases to 1.381 nm. The grafting of the organic moieties is difficult to address; it appears concomitantly with the reaction of polymerization. However, it takes place as underlined by the results gathered by S K-edge and FTIR spectroscopies, since any exchange reaction is unsuccessful.

At higher temperature, the textural properties and the morphologies are different. The presence of the organic component is found to delay the crystallization of the products of combustion, as reported for other related nanocomposites.[42]

After treatment at 473 K in air, the sample was left under air exposure at room temperature for 30 days. The intensity and the line width of the fine ESR signal increase significantly, ΔH_{pp} changing from 15 to 100 ± 10 G (Figure 11). Moreover, the g value changes from 2.0034 to 2.0060. Similar phenomenona were reported for the protonated emeraldine form of PANI[43] and for polypyrrole.[44] This was explained by the effect of physisorbed oxygen: a spin flip scattering with the O_2 paramagnetic molecules has been proposed in these cases. The initial ESR signal is recovered after vacuum treatment, showing that the reaction with oxygen at room temperature is reversible. In contrast to other systems,[41] it does not correspond to an intralamellar polymer growth.

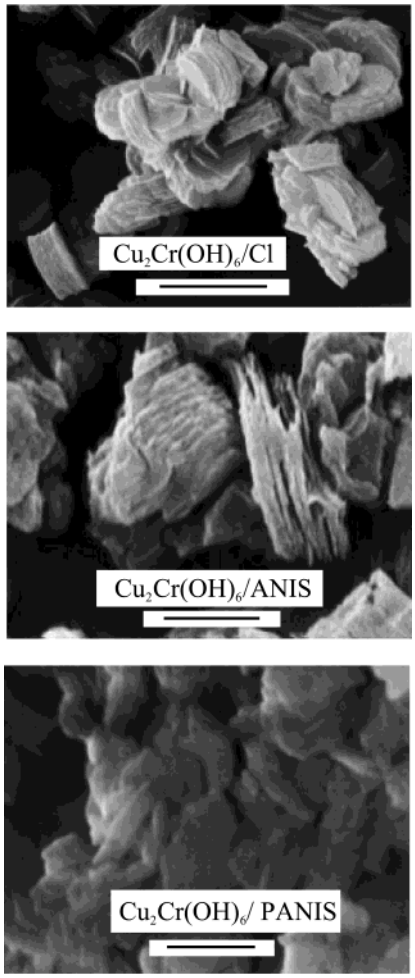

Figure 12. SEM pictures of (a) $Cu_2Cr(OH)_6$/Cl, (b) $Cu_2Cr(OH)_6$/ANIS, and (c) $Cu_2Cr(OH)_6$/PANIS. The bar represents 2 μm. Micrographs were recorded with a Cambridge Stereoscan 360 operating at 15 kV.

3.1.6. Air-Assisted Endotactic Reaction. SEM pictures provide an excellent example of topotactic reaction (Figure 12). Initially nicely stacked on each other, the layers are propped apart by the intercalation of monomers and left unmodified after the reaction of polymerization. The host structure sustains well the whole process. Supported by XRD and EXAFS techniques (vide supra), the accommodation may be explained by the good matching between the host structure and the monomeric repetition. To simplify the model, we consider the case of ideally packed hydroxyl groups lying in the galleries. In a same manner, the area per charge could be considered. The shorter distance between the successive charges is of $a\sqrt{3}$ (=5.38 Å for Cu_2Cr LDH compound) along the (100), (010), or (110) direction.[34] This is quite similar to the repetition of the monomer

(40) Bhuvanesh, N. S. P.; Gopalakrishnan, J. *Mater. Sci. Eng.* B **1998**, *53*, 267.
(41) Wu, C. G.; DeGroot, D. C.; Marcy, H. O.; Schindler, J. L.; Kannewurf, C. R.; Liu, Y. -J.; Hirpo, W.; Kanatzidis, M. G. *Chem. Mater.* **1996**, *8*, 1992. Liu, Y. -J.; DeGroot, D. C.; Schindler, J. L.; Kannewurf, C. R.; Kanatzidis, M. G. *J. Chem. Soc. Chem. Commun.* **1993**, 593. Bissessur, R.; DeGroot, D. C.; Schindler, J. L.; Kannewurf, C. R.; Kanatzidis, M. G. *J. Chem. Soc. Chem. Commun.* **1993**, 687. Liu, Y. -J.; Kanatzidis, M. G. *Inorg. Chem.* **1993**, *32*, 2989.
(42) Messersmith, P. B.; Stupp, S. *Chem. Mater.* **1995**, *7*, 454.
(43) Scott, J. C.; Pfluger, P.; Krounbi, M. T.; Street, G. B. *Phys. Rev. B* **1983**, *28*, 2140.
(44) Nakajima, H.; Matsubayashi, G. *Chem. Lett.* **1993**, 423.

(5.35 Å along the ...NH_2...NH_2 direction). From structural consideration, the host structure provides a strong confinement for the ANIS molecules (4.7 Å per molecule along the stacking direction) but supplies also a interlayer arrangement suitable for the polymerization.

It is reminiscent of the endotactic reaction between the PANI and FeOCl matrix.[45] In the PANI/FeOCl nanocomposite, the polymer orientation inside the solid is explained by the matching of two −NH− repetitions with the distance of chloride anions along the (101) direction. In our case, the resulting material does not present a superlattice structure. For the host structure, the ordered picture is available on small domains, as confirmed by the XAS study. For the polymer, it may result in the presence of short PANIS chains. The vibration bands at 710 and 620 cm^{-1}, characteristic of short-chain oligomers,[14] are consistent for this statement.

A preliminary study (two-probe conductivity) performed on pressed pellets of PANIS/Cu_2Cr shows no great measurable conductivity (less than 10^{-8} S cm^{-1}). Small conductive properties were reported for other PANI-related nanocomposites, $(PANI)_{0.80}Ca_2Nb_3O_{10}$ (less than 10^{-10} S cm^{-1}),[31] PANI/$HMMoO_6$ (M = Nb, Ta),[40] PANI/HUO_2PO_4,[46] or PANI/$VOPO_4$.[47] The lack of conductivity was explained by the fact that the polyaniline is encapsulated inside the inorganic host. Even if a part of the polymer presents metallic behavior, as exemplified with the ΔH_{pp} temperature dependence, the whole material does although not possess such a property. The polymer is present as isolated conductive domains (islands) dispersed in a nonelectronically conductive matrix or may also possess defects at its ends, as pointed out by Javadi et al.[48] In our case, a small conjugation length measured via an indirect method [49] associated to an electron-withdrawing effect of the sulfonate groups may cause a poor electronic delocalization.

4. Conclusion

Even if an oxidative polymerization of ANIS requires high-pressure conditions, the present paper shows that the ignition of the polymerization reaction may occur in the galleries of $Cu_2Cr(OH)_6Cl{\cdot}nH_2O$ LDH material under mild conditions. It requires simultaneously an air atmosphere and a confinement of the monomer molecules. EXAFS study shows that the host structure accommodates easily the incorporation and the polymerization. The soft treatment may be generalized to other monomer molecules as long as the conditions described above are met. It may also be enlarged to other LDH host structure.

Finally, we succeed to polymerize electrochemically the interleaved monomer ANIS in an aprotic solvent. The ESR signal in oxidation at 200 mV vs Pt is similar to the one obtained after the heat treatment in air. A complete study is under investigation.

Acknowledgment. The authors are grateful to Joël Cellier (LMI) for his assistance. We also thank Dr. Valérie Briois, Stéphanie Belin, and Anne-Marie Flank, for their help to acquire XAS spectra, and LURE, for the use of the facilities.

CM0211094

(45) Wu, C.-G.; DeGroot, D. C.; Marcy, H. O.; Schindler, J. L.; Kannewurf, C. R.; Bakas, T.; Papaefthymiou, V.; Hirpo, W.; Yesinowski, Y. P.; Liu, Y.-J.; Kanatzidis, M. G. *J. Am. Chem. Soc.* **1995**, *117*, 9229.

(46) Nakajima, H.; Matsubayashi, G. *Chem. Lett.* **1993**, 423.

(47) Kinomura, N.; Toyama, T.; Kumada, N. *Solid State Ionics* **1995**, *78*, 281.

(48) Javadi, H. H. S.; Laversanne, R.; Epstein, A. J.; Kholi, R. K.; Scherr, E. M.; Macdiarmid, A. G. *Synth. Met.* **1989**, *29*, E439.

(49) The extraction of the polymer from the LDH host material requires an acidic treatment, which may favor a polymer linkage reaction. The molecular weight determination (e.g., GPC) gives results that are not truly related to the interleaved polymer size.